

METHOD FOR DETERMINING A CONTINUOUS ABERRATION FREE HELIOSTAT SURFACE

Willem Landman¹ and Paul Gauché²

¹ MSc.Eng (Mechanical) Candidate, Dept. Mechanical and Mechatronic Engineering, Stellenbosch University, Private Bag X1, Matieland, 7602, South Africa, Phone: +27 84 400 2014, E-Mail: 16929098@sun.ac.za

² MEng (Mechanical), Sr. Researcher and Coordinator STERG, Dept. Mechanical and Mechatronic Engineering, Stellenbosch University

Abstract

A heliostat image that is small with a high flux density is advantageous. An image from a conventional spherically curved surface suffers from astigmatism for nonzero incidence angles. This aberration distorts and enlarges the resultant image leading to inefficiencies. A surface with different radii along the sagittal and coronal planes, as is found in a non-axial part of a paraboloid, will create an aberration free image. This paper presents a mathematical model using analytic expressions to calculate such a continuous reflective surface. The heliostat surface produces an aberration free image for a specified sun position and is described in a practical Cartesian coordinate system. Both azimuth-zenith tracking and target aligned tracking mechanisms are taken into account. The model is validated numerically against a geometric ray tracing model.

Keywords: heliostat; mirror surface; optics; aberration; focal spot; solar thermal

1. Introduction

This work forms part of a study of heliostat optics for the application to high temperature receivers where high flux densities are required.

The size of the flux map as well as the solar flux density from the heliostat field, are key design factors for a solar receiver. It is well documented and known fact from the second law of thermodynamics that increased receiver temperatures lead to increased efficiencies in the thermodynamic cycle [1] and that a smaller aperture area of the receiver leads to lower thermal losses [2]. It is, therefore, well known that a high flux density in a small flux map is advantageous.

In a power tower system, an array of heliostats individually tracks the sun in order to reflect the light to a static receiver located on a tower. The flux map at the receiver comprises of an accumulation of overlaid images created by individual heliostats. By decreasing the size of the images cast by individual heliostats the size of the flux map at the receiver (hereafter referred to as the target) can be reduced and higher flux densities achieved.

A heliostat with a flat mirror surface creates an image the size of the normal projection increased by 9.3 mrad of sun spread [3], as seen in Figure 1. Such an image is large and can be reduced in size down to only 9.3 mrad of sun spread by using a curved mirror surface. Typically a spherical shape is used where curvature r is constant over the surface. The radius of curvature is selected for a given focal length $f = r/2$ where the focal length is the distance from the heliostat to the tower.

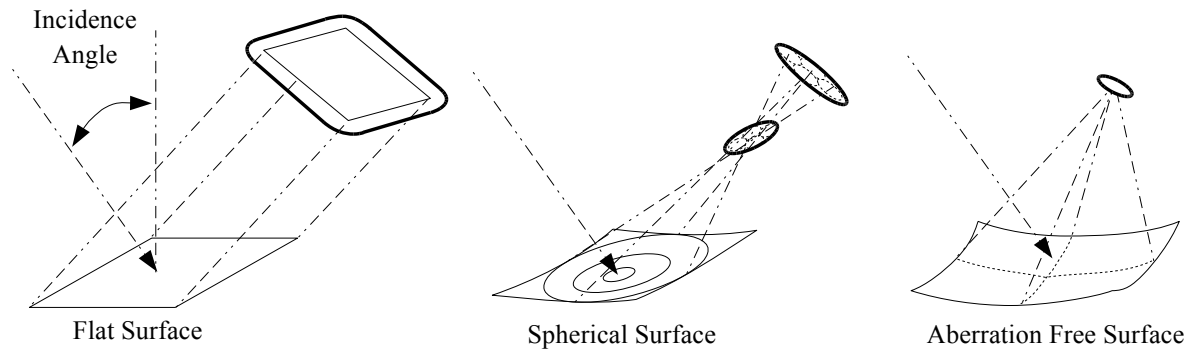


Fig. 1. Resulting Images for Different Heliostat Surfaces Shapes

A spherically curved mirror surface is acceptable in the event that the heliostat, target and sun are collinear or have a zero incidence angle [4]. This, however, is not the case since the surface normal does not point towards the sun but rather points towards the bisector of the vectors to the sun and target. This means that a heliostat never has a zero incidence angle.

Spherically curved mirror surfaces suffer from astigmatism for nonzero incidence. This aberration is responsible for image distortion by spreading the image over a larger area and makes a sharp image impossible [4]. Ingel and Hughes [5] showed that aberration increases with increased incidence angles.

Many authors that have attempted to address these problems. Ingel and Hughes realised that aberration can be reduced by asymmetric curvature [5]. This requires that the heliostat be aligned with the coronal plane, also referred to as the tangential plane. Ries and Zaibel [4, 6] have suggested a new tracking mechanism that aligns the heliostat to the coronal plane using spin and elevation tracking known as target aligned tracking, depicted in Figure 2. Target aligned tracking allows the required curvature in one direction to remain unchanged resulting in the elimination of first order aberration. Chen [7] suggested a reduction of second order aberration with the use of a dynamic non-imaging heliostat, utilizing target aligned tracking. Here slave mirrors would adjust the focal length in the sagittal plane dynamically.

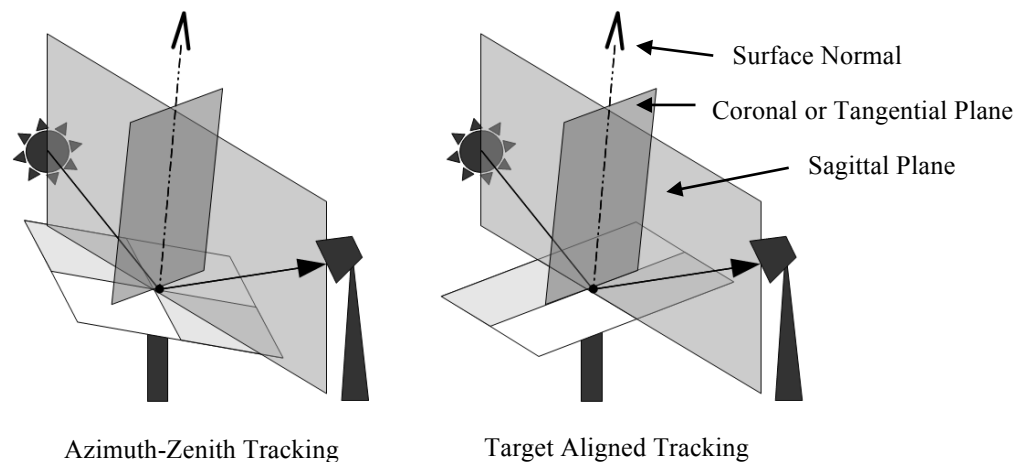


Fig. 2. Optical Planes of Azimuth-Zenith and Target Aligned Tracking Mechanisms

Although the proposed solutions to astigmatism have proven invaluable and are capable of practical implementation [8], the essence of the problem has not been fully addressed. Only first order aberration have been corrected by using the target aligned tracking mechanism and second order aberration have been reduced by using a dynamic non-imaging surface. Full aberration correction has not been proposed.

There, does, however exist one surface that will create an aberration free image. That surface must have variable radii along the sagittal and coronal planes as is found in a non-axial part of a paraboloid. This was

noted by Zaibel in 1995 [4] but thereafter ignored by literature. It is appropriate to mention here that full correction is only possible using a dynamic heliostat surface since the required curvature is dependent on the ever changing sun position. The model presented in this paper formulates a continuous, theoretical surface using analytical expressions, to produce an aberration free image for a specified sun position.

The intention of the model was to create the theoretical ideal optics of a heliostat as part of further research into heliostat optics. Practical application the model is limited to an ideal optical surface shape at a specific moment in time but can be extended to a dynamic heliostat. Such a heliostat will require a method to accurately deform a continuous reflective surface in three dimensions with time.

2. Mathematical Model

The surface that will create an aberration free image is found in the non-axial part of a paraboloid. A spherical paraboloid has the well-known geometric property that incidence rays, parallel to the axis of revolution, are reflected to a single point, known as the focal point.

Assume a hypothetical paraboloid surface is created where the target is placed at the focal point and the axis of revolution is toward the sun, as depicted in Figure 3. Specular reflection from any part of the surface will create an aberration free image at the target. Thus if a heliostat mirror surface forms part of this paraboloid it will also create an aberration free image at the target. Even though a paraboloid is easily defined a description of the surface using a practical coordinate system at the heliostat is required.

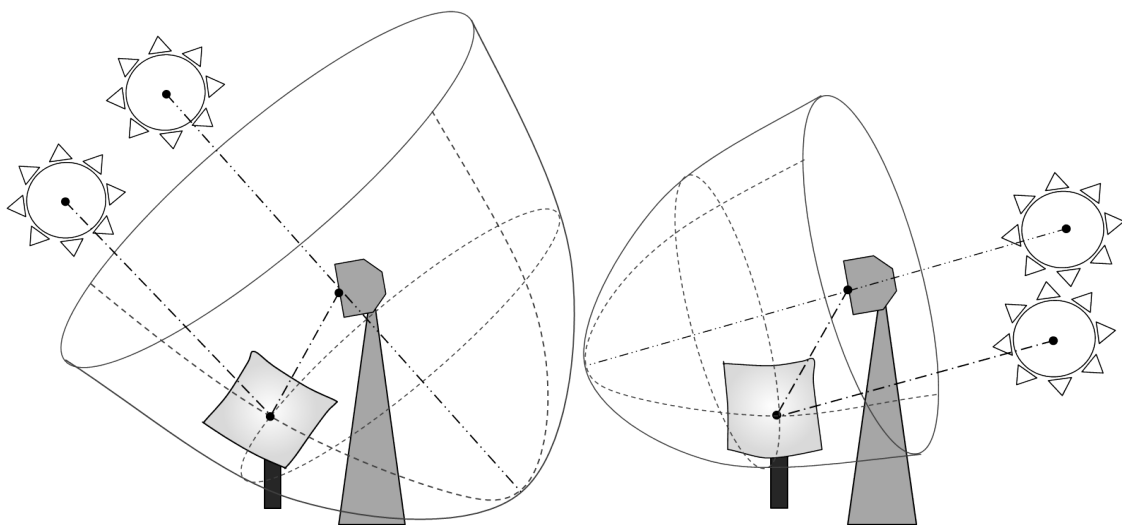


Fig. 3. Hypothetical Paraboloid for Different Sun Positions

Within the model a hypothetical paraboloid is defined and mathematically manipulated in order to describe the resultant theoretical surface in a practical coordinate system. The model is described in detail below.

2.1. Inputs

At the outset three variables are finite;

- the position of the sun that can be determined through numerous methods [9, 10, 11]
- the physical position of the target
- the physical position of the heliostat

Since the model will result in a continuous equation that describes the surface, the dimensions of the heliostat do not need to be specified.

2.2. Coordinate systems

In order to simplify the calculation four different Cartesian coordinate systems, shown in Figure 4, are defined;

1. Paraboloid coordinate system (PCS): A coordinate system with its origin is the centre of the target and with the Z axis aligned pointing toward the sun collinear to the paraboloid rotation axis.
2. Target coordinate system (TCS): A coordinate system where its origin is the same as that of the PCS, where the X and Y axis are defined by Geographic North and East and the Z axis the resulting vertical.
3. Heliostat coordinate system (HCS): A coordinate system with the same axis definition to the target coordinate system but where the origin is in the centre point of the heliostat surface.
4. Mirror surface coordinate system (MCS): A practical coordinate system in which the surface will be described. The origin is at the centre of the heliostat surface, where the Z axis is the heliostat normal (pointing direction) and the X and Y axes are defined by the edges of a rectangular heliostat.

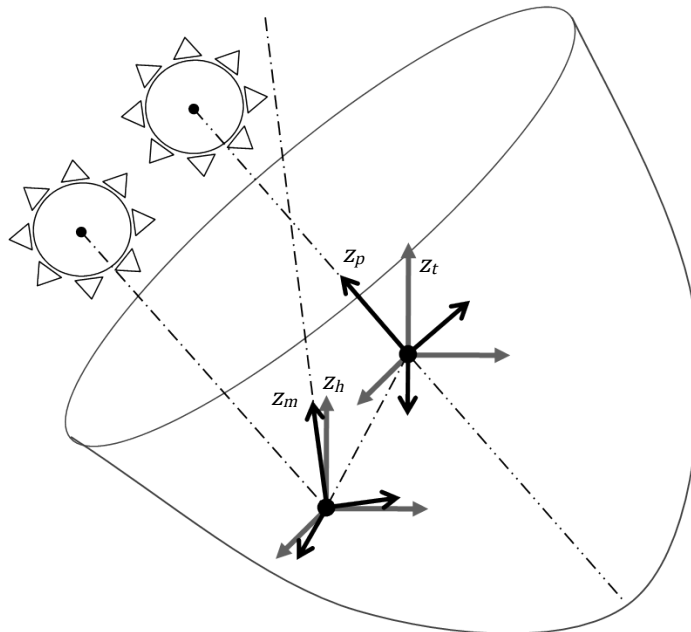


Fig. 4. Axis Systems

2.3. Defining the Paraboloid

It is known that incoming rays parallel to the axis of rotation are reflected to the origin by a paraboloid surface defined in the PCS.

$$z_p = (x_p^2 + y_p^2)/(4f) - f \quad (1)$$

By describing the heliostat position in the PCS, the focal length of the paraboloid f can be solved for by substituting the coordinates into Equation 1.

2.4. Transformation of Coordinate Systems

The surface is now defined in PCS, however it is desired that the surface be described in MCS. In order to convert the surface a transformation between coordinate systems needs to be performed. In order to simplify the problem the transformation is done in parts and collated later in Equation 12.

First a transformation matrix from PCS to TCS, Q_{pt} , is required. This is a rotation only since the origins are common. A rotation matrix is calculated using the Rodrigues' rotation formula, which rotates a vector in

space around a given axis u , in unit vector, form by angle θ in a right handed sense.

$$Q = I \cos \theta + [\mathbf{u}]_{\times} \sin \theta + (1 - \cos \theta) \mathbf{u} \otimes \mathbf{u} \quad (2)$$

where $\mathbf{u} \otimes \mathbf{u}$ is the tensor product

$$\mathbf{u} \otimes \mathbf{u} = \begin{bmatrix} u_x^2 & u_y u_x & u_z u_x \\ u_x u_y & u_y^2 & u_z u_y \\ u_x u_z & u_y u_z & u_z^2 \end{bmatrix} \quad (3)$$

and where $[\mathbf{u}]_{\times}$ is the cross product matrix

$$[\mathbf{u}]_{\times} = \begin{bmatrix} 0 & -u_z & u_y \\ u_z & 0 & -u_x \\ -u_y & u_x & 0 \end{bmatrix} \quad (4)$$

The axis of rotation u is found using the normalised cross product of the z-axis's and the rotation angle θ is the arccosine of the dot product of the z-axis 's.

Now that the surface can be transformed to the TCS a transformation matrix to HCS is required. Since the HCS is a linear displacement of TCS, a translation can be used which adds the vector of the heliostat relative to the target, \mathbf{h} , to the surface vector.

$$T_h\{\mathbf{v}\} \quad \text{or} \quad \mathbf{v} + \mathbf{h} \quad (5)$$

A second rotation only transformation matrix from HCS to MCS, Q_{hm} , is calculated using Rodrigues' rotation formula similar to Q_{pt} discussed in detail above.

Finally a transformation matrix to take into account the tracking mechanisms used, Q_T , is found. At this point of the calculation the surface is already described in the correct coordinate system, however due to different tracking configurations the X and Y axis, previously defined as the edges of a rectangular heliostat, are misaligned. Again the Rodrigues' rotation formula can be used. The axis of rotation \mathbf{u} is given as the Z axis, whilst the rotation angle θ is dependent on the tracking mechanism used. Two tracking mechanisms were considered namely azimuth-zenith tracking and target aligned tracking which are discussed individually below.

2.4.1. Azimuth-zenith tracking

During tracking the projection of the Y axis onto the geographical ground plane must be collinear with the projection of the surface normal or bisection vector at the origin onto the ground plane. This is achieved by projecting the bisection vector in the HCS, \mathbf{b} , onto the geographic X Y plane.

$$\mathbf{v}_h = \mathbf{b} \times \begin{pmatrix} 0 \\ 0 \\ 1 \end{pmatrix} \times \mathbf{b} \quad (6)$$

The resulting vector, \mathbf{v}_h , is transformed to MCS using the transformation matrix Q_{hm} previously calculated.

$$\mathbf{v}_m = Q_{hm} \mathbf{v}_h \quad (7)$$

This vector, \mathbf{v}_m , is then projected onto the X Y axis of the MCS

$$\mathbf{v}_p = \begin{pmatrix} 0 \\ \mathbf{v}_m \times 0 \times \mathbf{v}_m \\ 1 \end{pmatrix} \quad (8)$$

Here after the rotation angle θ can then be calculated by the arccosine of the dot product between the X axis and the projection onto the X Y plane, \mathbf{v}_p .

$$\theta = \cos^{-1} \left(\begin{pmatrix} 1 \\ 0 \\ 0 \end{pmatrix} \cdot \mathbf{v}_p \right) \quad (9)$$

2.4.1. Target aligned tracking

During target aligned tracking the X axis remains on the coronal plane. The rotation is thus from the X axis to the projection of the incidence ray \mathbf{d}_i onto the X Y plane.

$$\mathbf{v}_p = \begin{pmatrix} 0 \\ \mathbf{d}_i \times 0 \times \mathbf{d}_i \\ 1 \end{pmatrix} \quad (10)$$

The rotation angle θ can then be calculated by the arccosine of the dot product between the X axis and the projection onto the X Y plane.

$$\theta = \cos^{-1} \left(\begin{pmatrix} 1 \\ 0 \\ 0 \end{pmatrix} \cdot \begin{pmatrix} 0 \\ \mathbf{d}_i \times 0 \times \mathbf{d}_i \\ 1 \end{pmatrix} \right) \quad (11)$$

2.5. Surface Transformation

The surface vector in PCS, \mathbf{v}_p , is thus described by a surface vector in MCS, \mathbf{v}_m . Each element of the paraboloid surface vector \mathbf{v}_p is described by the elements of the surface vector, \mathbf{v}_m .

$$\mathbf{v}_p = Q_{pt} T_h \{ Q_{hm} Q_T \mathbf{v}_m \} \quad (12)$$

Substituting the elements of \mathbf{v}_p into Equation 1 and solving for z_m we can describe the mirror surface in the MCS.

$$z_m = ax_m + b + cy_m + d(ex_m^2 + fx_m + gx_my_m + h + iy_m^2 + j)^{1/2} \quad (13)$$

where symbols a to j are constants. It is important to note here that two solutions exist and that the solution where d is negative should be used in order to avoid the roof of the parabola.

Equation 13 is a theoretical, continuous, heliostat mirror surface, described in a practical coordinate system (MCS) that will create an aberration free image at the defined target. The surface is depicted in Figure 5 below.

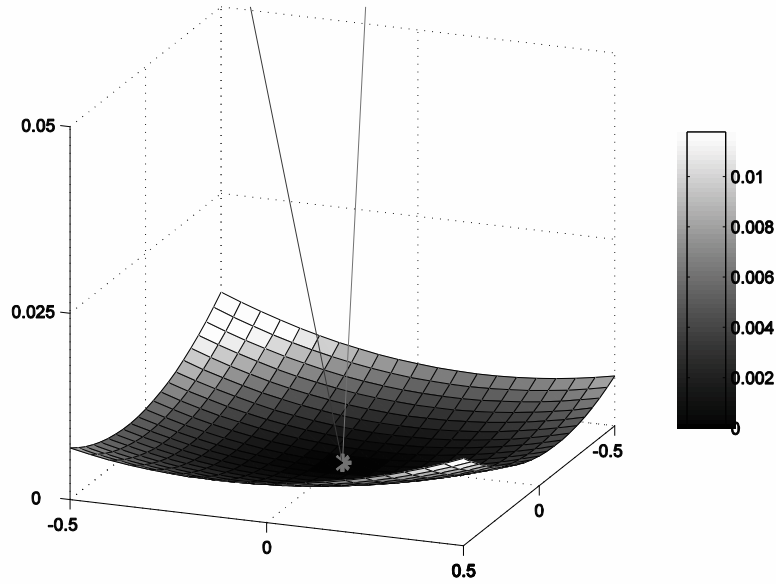


Fig. 5. Exaggerated view of the Mirror Surface using AZ tracking

3. Validation

The model is validated numerically against a geometric ray tracing model. Light is reflected specularly off the resulting surface, described by Equation 13. A cone of light dependent on the sun shape is reflected from an infinitesimal point. Only the symmetry axes of the reflected cones need to be considered since the centres of all the images reflected from the infinitesimal points will collate at the point where these axes meet. If all the rays, reflected about the surface normals, pass through a single point at the target it can be concluded that the equation describes an aberration free mirror surface.

The normal to the surface is defined as the cross product of the partial differentials.

$$\mathbf{d}_n(x, y) = \begin{bmatrix} 1 \\ 0 \\ \frac{dz}{dx} \end{bmatrix} \times \begin{bmatrix} 0 \\ 1 \\ \frac{dz}{dy} \end{bmatrix} \quad (14)$$

Since the surface normal and incidence ray is known the reflected ray can be calculated.

$$\mathbf{d}_r = 2(\mathbf{d}_n \cdot \mathbf{d}_i)\mathbf{d}_n - \mathbf{d}_i \quad (15)$$

Figure 6 shows a visual representation of the reflectance.

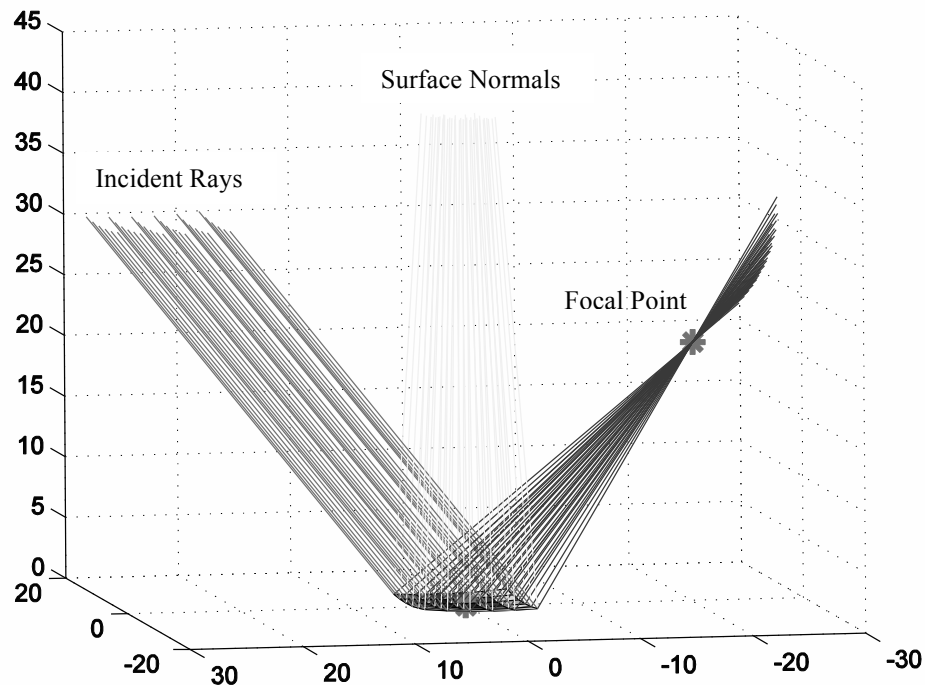


Fig. 6. Example of Validation

4. Conclusion

A small high flux density focal spot is advantageous. Conventional curved heliostats surfaces suffer from aberration losses which increase focal spot size. A surface with different radii along the sagittal and coronal planes as is found in a non-axial part of a paraboloid will create an aberration free image. A mathematical model is presented that uses analytical expressions to create a continuous heliostat surface in a practical coordinate system. The surface produces an aberration free image for a specified sun position. Both azimuth zenith tracking and target aligned tracking mechanisms are taken into account. The model is validated numerically with a geometric ray tracing model which is also presented.

Acknowledgements

We acknowledge with thanks the support for this work by the Solar Thermal Energy Research Group that made funds available through the solar spoke of the Department of Science and Technology, the National Research Fund and the Stellenbosch University Hope Project. We gratefully acknowledge the advice received from Dr M.F. Maritz from Stellenbosch University Applied Mathematics.

References

- [1] A. Segal, M. Epstein, Optimized working temperatures of a solar central receiver, *Solar Energy*, 75 (2003) 503 - 510.
- [2] A. Segal, M. Epstein, Comparative performances of 'Tower-Top' and 'Tower-Reflector' central solar receivers, *Solar Energy*, 65 (4) (1999) 207 - 226.
- [3] L E. Parrott, Theoretical upper limit to the conversion efficiency of solar energy, *Solar Energy*, 21 (1978) 227 - 229

- [4] R. Zaibel, E. Dagan, J. Karni, H. Ries, An astigmatic corrected target-aligned heliostat for high concentration, *Solar Energy Materials and Solar Cells*, 37 (1995) 191 - 202.
- [5] E.A. Igel, R. L. Hughes, Optical Analysis of Solar Facility Heliostat, *Solar Energy*, 22 (1979) 283 - 295.
- [6] H. Ries, M. Schubnell, The optics of a two-stage Solar furnace, *Solar Energy Materials*, 21 (1990) 213 - 217.
- [7] Y. T. Chen, K.K. Chong, T.P. Bligh, L.C. Chen, J. Yunus, K. S. Kannan, B.H. Lim, C.S. Lim, M.A. Alias, N. Bidin, O. Aliman, S. Salehan, Shk. Abd. Rezan S.A.H., C.M. Tam, K.K. Tan, Non-imaging focusing heliostat, *Solar Energy*, 71 (3) (2001) 155 - 164.
- [8] Y. T. Chen, A. Kribus, B. H. Lim, C. S. Lim, K.K. Chong, J. Karni, R. Buck, A. Pfahl, T.P. Bligh, Comparison of Two Sun Tracking Methods in the Application of a Heliostat Field, *ASME Journal of Solar Energy*, 126 (2004) 638 - 644.
- [9] J.J. Michalsky, The astronomical almanac's algorithm for approximate solar position (1950-2050), *Solar Energy*, 40 (3) (1988) 227 - 235.
- [10] I. Reda, A. Andreas, Solar position algorithm for solar radiation applications, *Solar Energy*, 76 (2004) 577 - 589.
- [11] M. Blanco-Muriel, D.C. Alarcon-Padilla, T. Lopea-Moratalla, M. Lara-Coira, Computing the solar vector. *Solar Energy*, 70 (5) (2001) 431 - 441.